Preprints of the 21st IFAC World Congress (Virtual)
Berlin, Germany, July 12-17, 2020

Performance–guaranteed consensus control inspired by the mammalian limbic system for a class of nonlinear multi-agents ⋆

Ignacio Rubio Scola *,**
Luis Rodolfo Garcia Carrillo, *Member, IEEE* **
João P. Hespanha, *Fellow, IEEE* *** Rogelio Lozano ****

* *CIFASIS (CONICET-UNR) and Department of Mathematics, National University of Rosario, Rosario, 2000, Argentina. (e-mail: irubio@fceia.unr.edu.ar).*
** *Unmanned Systems Laboratory. School of Engineering and Computer Sciences, Texas A&M University - Corpus Christi, Texas, USA. 78412-5797. (e-mail: luis.garcia@tamucc.edu)*
*** *Center for Control, Dynamical Systems, and Computation, University of California, Santa Barbara, CA 93106, USA. (e-mail: hespanha@ucsb.edu)*
**** *Heuristique et Diagnostic des Systèmes Complexes, Université de Technologie de Compiègne, UMR CNRS 7253, 60200 Compiègne, France (e-mail:rogelio.lozano@hds.utc.fr).*

Abstract: Computational models of emotional learning observed in the mammalian brain have inspired diverse self-learning control approaches. These architectures are promising in terms of their fast learning ability and low computational cost. In this paper, the objective is to establish performance–guaranteed emotional learning–inspired control (ELIC) strategies for autonomous multi–agent systems (MAS), where each agent incorporates an ELIC structure to support the consensus controller. The objective of each ELIC structure is to identify and compensate model differences between the theoretical assumptions taken into account when tuning the consensus protocol, and the real conditions encountered in the real system to be stabilized. Stability of the closed-loop MAS is demonstrated using a Lyapunov analysis. Simulation results based on the consensus task of a group of inverted pendulums demonstrate the effectiveness of the proposed ELIC for stabilization of nonlinear MAS.

Keywords: Multi-agents systems, Biologically-inspired control, Robust control, Distributed control, Nonlinear Control.

1. INTRODUCTION

The idea of *consensus* is an important research problem arising from the domain of distributed control of multi-agent system (MAS). The objective of this methodology is to design distributed control laws based on local relative information, in order to guarantee a stable agreement between the states of the agents. Most of the literature in this area has primarily addressed MAS with double-integrator dynamics, see for example Ren and Beard (2008), Pilloni et al. (2013), and Long et al. (2018). Along these lines, the problem of global robust distributed output consensus of heterogeneous leader–follower nonlinear MAS is widely studied, e.g., Xu et al. (2016) and Chen and Zhao (2018). In a real–world scenario, however, coordination of MAS is challenging because the dynamics of the robotic agents, which could be aerial, ground, water vehicles, or even a combination of them, are usually not precisely known. Furthermore, MAS that execute missions in unstructured/uncertain environments are often subject to disturbances and varying operational conditions.

In recent years, computationally complex control engineering problems have been solved using biologically-inspired solutions. In Moren (2002), a computational model known as Brain Emotional Learning (BEL) was developed, which mimics parts of the brain that are known to produce emotion. The BEL framework can be used for control systems purposes as in Lucas et al. (2004), where the authors develop a BEL–Based Intelligent Controller (BELBIC) which imitates the emotional parts of the mammalian brain, namely, the amygdala, the orbitofrontal cortex (OFC), the thalamus, and the sensory input cortex. Classic control methodologies may require the knowledge of all the dynamics of the model to be controlled. BELBIC, as a model-free controller, has no such a requirement. Furthermore, BELBIC has a single-layered architecture and therefore its computational complexity is in the order of $O(n)$, which is relatively small if compared to other existing learning-based intelligent controls, and therefore more appealing for real-time implementation.

⋆ This work was supported by ARO under grant W911NF1810210 and by NSF under grant EPCN-1608880.

Copyright lies with the authors

In our recent work, we proposed and implemented a tracking controller for an unmanned aircraft systems (UAS) Jafari et al. (2018) and for a MAS Jafari et al. (2017a), Jafari et al. (2017b) in the presence of uncertain system dynamics and disturbances using a BEL-inspired flocking controller. In contrast to these works, we now propose a biologically-inspired controller for each agent in order to imitate double integrator dynamics, and then reuse techniques for double integrator consensus. Furthermore, we propose a novel technique for improving the MAS trajectory tracking task, ensuring the inter-agent distance is maintained at the desired values, even in the presence of external disturbances. Our goal is to demonstrate that the implementation of an emotional learning-inspired control (ELIC) can stabilize a MAS in terms of consensus, trajectory tracking, and disturbance rejection.

The rest of the paper is organized as follows. Background on ELIC control is provided in Section 2, together with our main result, the double integrator closed-loop imitation ELIC controller. Next, Section 3 revisits consensus techniques for agents with double integrator dynamics, and introduces an original novel technique for achieving improved repulsion between agents. The performance analysis of the proposed MAS consensus control is provided in Section 4 by means of numerical results. Section 5 concludes the paper and provides current and future directions of this research.

2. EMOTIONAL LEARNING-INSPIRED CONTROL

Consider an agent whose dynamic model is consistent with a class of nonlinear systems of order n described by

$$x^{(n)} = f(\underline{x}) + g(\underline{x})u + d(\underline{x}, t) \tag{1}$$

where $\underline{x} = [x, \dot{x}, \ldots, x^{(n-1)}]^T \in \mathbb{R}^n$ is the state vector, $\dot{x}$ is the derivative of x w.r.t. time, $x^{(n-1)}$ is the $(n-1)^{\text{th}}$ ordered derivative of x w.r.t. time, and $u \in \mathbb{R}$ is the control input. Assume the vector state $\underline{x}$ belongs to the compact set $\Omega_x = \{\underline{x} \mid \|\underline{x}\| \le M_x\}$ with M_x a positive constant. Assume also that $g(\underline{x}) > 0$, and $g(\underline{x})^{-1}$ and $f(\underline{x})$ are unknown continuous scalar functions.

Assume that the desired trajectory x_d and its derivatives, up to its n^{th} order derivative, are smooth and bounded.

Let's define an auxiliary variable s depending on the system's tracking error and its derivatives as

$$s = e^{(n-1)} + \Delta_{n-1}e^{(n-2)} + \ldots + \Delta_1 e \tag{2}$$

with the tracking error $e = x - x_d$, and Δ_k $(k = 1, 2, \ldots n-1)$ are constants such that the roots of the polynomial $\lambda^{n-1} + \Delta_{n-1}\lambda^{n-2)} + \ldots + \Delta_1 = 0$ have negative real part.

If $f(\underline{x})$ and $g(\underline{x})$ were known and $d(\underline{x}, t) = 0$, it would be possible to achieve the dynamics $\dot{s} = -Ks + u_r$ with the following exact matching control law

$$u^* = -g^{-1}(\underline{x})(f(\underline{x}) + q_a + Ks - u_r), \tag{3}$$

with $q_a = -x_d^{(n)} + e^{(n-1)} + \Delta_{n-1}e^{(n-2)} + \ldots + \Delta_1\dot{e}$, and u_r as an auxiliary input that will be specified below.

Note that the assumptions of boundedness of $\underline{x}$, $f(\cdot)$, $g^{-1}(\cdot)$, x_d, and its derivatives up to order n, ensure that the exact matching controller is bounded.

In Rubio Scola et al. (2020), an improvement on the performance of the system can be accomplished through an integral action. To this end, a new state $\xi(t) = \int s(t)dt$ is introduced and s is extended as $s_e = [s,\ \xi]^T$ leading to

$$\begin{bmatrix}\dot{s}\\ \dot{\xi}\end{bmatrix} = \underbrace{\begin{bmatrix}-K & 0\\ 1 & 0\end{bmatrix}}_{A_e}\begin{bmatrix}s\\ \xi\end{bmatrix} + \underbrace{\begin{bmatrix}1\\ 0\end{bmatrix}}_{B_e}u_r \tag{4}$$

The auxiliary innput term u_r can be obtained by solving the Ricatti equation

$$0 = A_e^T P_e + P_e A_e - P_e B_e R^{-1} B_e^T P_e + Q_e \tag{5}$$

$$u_r = -\frac{1}{r} B_e^T P_e s_e \tag{6}$$

where $Q_e = \text{diag}\{Q, Q_I\}$ and $R = \frac{\rho^2 r}{2\rho^2 - r}$, with $Q_e = Q_e^T \succ 0$ and $2\rho^2 > r$.

To approximate the unknown functions $f(\underline{x})$ and $g(\underline{x})$ by means of estimates $\hat{f}(\underline{x})$ and $\hat{g}(\underline{x})$ we propose a combination of Gaussian Radial Basis Functions (RBF) that emulates the emotional learning structure of the mamial limbic system (see Moren (2002) for details):

$$\begin{aligned}\hat{f}(\underline{x}) :=& \hat{f}(\underline{x}, V_f, W_f) = V_f^T \Phi_A(s(\underline{x})) - W_f^T \Phi(s(\underline{x}))\\ \hat{g}(\underline{x}) :=& \hat{g}(\underline{x}, V_g, W_g) = V_g^T \Phi_A(s(\underline{x})) - W_g^T \Phi(s(\underline{x}))\end{aligned} \tag{7}$$

where

$$\begin{aligned}V_f &= [V_{f1}, V_{f2}, \ldots, V_{fp}, V_{f\text{th}}]^T,\\ W_f &= [W_{f1}, W_{f2}, \ldots, W_{fp}]^T,\\ V_g &= [V_{g1}, V_{g2}, \ldots, V_{gp}, V_{g\text{th}}]^T,\\ W_g &= [W_{g1}, W_{g2}, \ldots, W_{gp}]^T\end{aligned}$$

are vectors of weight parameters. The terms Φ_j^{th} are Gaussian RFB's that can be represented using the structure

$$\begin{aligned}\Phi_j &= \exp\left(-\frac{(s-\mu_j)^2}{\sigma_j^2}\right),\\ m &= \max([\Phi_1, \Phi_2, \ldots, \Phi_p])\end{aligned} \tag{8}$$

where s is the error dynamics described by equation (2), and μ_j and σ_j are the corresponding mean and smoothing factor, respectively. The RBF are $\Phi = [\Phi_1, \Phi_2, \ldots, \Phi_p]^T$ and $\Phi_A = [\Phi, m]^T$, m is the input from Thalamus, and V_{th} is its corresponding weight.

Let the optimal weight parameters be defined as follows

$$[V_f^*, W_f^*] = \underset{V_f \in \Omega_{fv}, W_f \in \Omega_{fw}}{\arg\min} [\sup_{\tilde{\underline{x}} \in \Omega_x} |V_f^T \Phi_A(\tilde{\underline{x}}) - W_f^T \Phi(\tilde{\underline{x}}) - f(\tilde{\underline{x}})|], \tag{9}$$

$$[V_g^*, W_g^*] = \underset{V_g \in \Omega_{gv}, W_g \in \Omega_{gw}}{\arg\min} [\sup_{\tilde{\underline{x}} \in \Omega_x} |V_g^T \Phi_A(\tilde{\underline{x}}) - W_g^T \Phi(\tilde{\underline{x}}) - g(\tilde{\underline{x}})|], \tag{10}$$

The notation $\hat{f}^*(\underline{x}) := \hat{f}(\underline{x}, V_f^*, W_f^*)$ and $\hat{g}^*(\underline{x}) := \hat{g}(\underline{x}, V_g^*, W_g^*)$ will be used in the following for simplicity.

The errors of the approximation functions w.r.t. the real value are defined as

$$\begin{aligned}f_e(\underline{x}) =& f(\underline{x}) - \hat{f}^*(\underline{x}), \qquad g_e(\underline{x}) = g(\underline{x}) - \hat{g}^*(\underline{x}),\\ \tilde{\omega} =& f_e(\underline{x}) + g_e(\underline{x})u\end{aligned} \tag{11}$$

and the weight estimation errors as

$$\tilde{V}_f = V_f^* - V_f \qquad \tilde{V}_g = V_g^* - V_g$$
$$\tilde{W}_f = W_f^* - W_f \qquad \tilde{W}_g = W_g^* - W_g \tag{12}$$

We use the same adaptation rules as presented in Rubio Scola et al. (2020)

Assumption 1. The optimal adaptive parameters V_f^*, W_f^*, V_g^*, and W_g^* belong to the following compact sets, respectively: $\Omega_{fv} = \{V_f^* | \|V_f^*\| \leq M_{fv}\}$, $\Omega_{fw} = \{W_f^* | \|W_f^*\| \leq M_{fw}\}$, $\Omega_{gv} = \{V_g^* | 0 < \delta \leq \|V_g^*\| \leq M_{gv}\}$, and $\Omega_{gw} = \{W_g^* | 0 < \delta \leq \|W_g^*\| \leq M_{gw}\}$. Here, δ, M_{fv}, M_{fw}, M_{gv}, and M_{gw} are positive constants.

The following theorem can now be formulated.

Theorem 1. (ELIC Theorem). [Rubio Scola et al. (2020)] Consider the nonlinear system in equation (1) with the following control law

$$u = -\hat{g}^{-1}(\underline{x})(\hat{f}(\underline{x}) + q_a + Ks - u_r) \tag{13}$$

where $\hat{f}$ and $\hat{g}$ are given by equation (7), with BEL-inspired adaptation laws as described in Rubio Scola et al. (2020) , and u_r as defined in equation (6). Under this scenario, the H_∞ tracking performance criteria described in equation (14) is fulfilled for a pre-given attenuation level ρ, and the error function s remain bounded

$$\int_0^T s_e^T Q_e s_e dt \leq \frac{1}{\alpha_f}\tilde{V}_f(0)^T\tilde{V}_f(0) + \frac{1}{\beta_f}\tilde{W}_f(0)^T\tilde{W}_f(0)$$
$$+ \frac{1}{\alpha_g}\tilde{V}_g(0)^T\tilde{V}_g(0) + \frac{1}{\beta_g}\tilde{W}_g(0)^T\tilde{W}_g(0)$$
$$+ s_e^T(0)P_e s_e^T(0) + \rho^2\int_0^T \omega^T\omega dt \tag{14}$$

2.1 ELIC for MAS consensus

In terms of MAS consensus, the main objective is to design a control signal u_i for each agent i, in such a way that the motion of all agents in the MAS exhibits an *emergent behavior* arising from simple rules that are followed by individuals, and does not involve any central coordination.

For the novel framework proposed here, each i^th agent will incorporate an ELIC$_i$ structure to support the consensus controller. The objective of each ELIC$_i$ control structure is to identify and compensate model differences between what was theoretically supposed when tuning the MAS controllers (see eqs. (25)-(27)) and the real practical conditions. Despite using a linear model for each agent (see the MAS dynamics in equation (20)), the interconnection of the agents is done with a nonlinear MAS protocol (see eqs. (25)-(27)). This leads to a nonlinear propagation of the MAS model uncertainties or external perturbations. In the absence of model mismatch and/or disturbances, the ELIC should not interfere with the nominal MAS control. The novel framework interfaces the ELIC controller with the MAS, by implementing a reference model of a double integrator to create a virtual reference for the s variable. The proposed interconnection framework, which we call *Double Integrator*–ELIC (DIELIC) is shown in Fig. 1. Such system is composed by an agent in closed-loop with an ELIC, imitating double integrator dynamics.

2.2 Double integrator closed-loop behaviour

We propose to use the ELIC to compensate the differences between the model of each agent and a nominal system described by a double integrator. This facilitates the implementation of consensus theory designed for second order nonlinear agents controlled by means of ELIC.

Let's consider a reference model representing the double integrator dynamics

$$\ddot{x}_d = u_{DI} \tag{15}$$

where the subscript $(\cdot)_{DI}$ indicates the Double Integrator system that the ELIC closed-loop should imitate.

Next, the system output is compared with the reference model that represents the double integrator dynamics:

$$e = x_d - y \tag{16}$$
$$x^{(n)} = f(\underline{x}) + g(\underline{x})(u_{DI} + u_{ELIC}) \tag{17}$$

where u_{ELIC} comes from the controller in eq.(13) and u_{DI} is defined in eq.(15).

The DIELIC closed-loop system can now be rewritten as

$$x^{(n)} = f(\underline{x}) + g(\underline{x})u_{ELIC} + \underbrace{g(\underline{x})u_{DI} - u_{DI}^{(n-2)}}_{d(\underline{x},t)} + u_{DI}^{(n-2)} \tag{18}$$

The stability proof, which derives from Theorem 1, is omitted here for brevity.

For the particular case of a second order system we have

$$\ddot{x} = f(\underline{x}) + g(\underline{x})u_{ELIC} + g(\underline{x})u_{DI} - u_{DI} + u_{DI} \tag{19}$$

if $f(x) = 0$ and $g(x) = 1$, the systems (15) and (19) are identical. If both systems have the same initial conditions, there is no need for compensation and the ELIC controller output should be $u_{ELIC} = 0$.

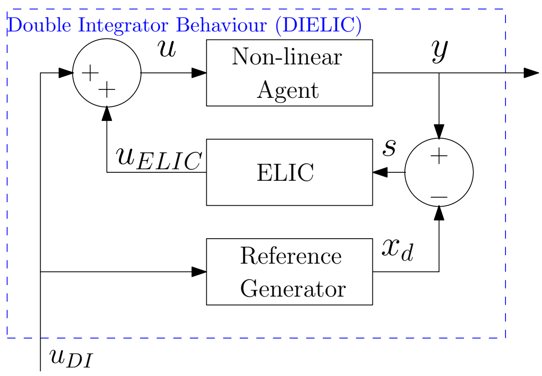

Fig. 1. DIELIC structure: an ELIC imitating the double integrator behaviour.

With the DIELIC imitating double integrator agents, we can directly apply consensus techniques for double integrator agents. Hereafter, we revisit relevant results for MAS consensus with double integrator agents.

3. CONSENSUS FOR AGENTS WITH DOUBLE INTEGRATOR DYNAMICS

Assuming n agents with second order dynamics evolving in an m dimensional space ($m = 2, 3$), it is possible to describe the motion of each agent i as

$$\dot{q}_i = p_i, \quad \dot{p}_i = u_i, \quad i = 1, 2, \ldots, n \tag{20}$$

where $\{u_i,\ q_i,\ p_i\} \in \mathbb{R}^m$ are control input, position, and velocity of agent i, respectively. An associated dynamic graph $G(\upsilon, \varepsilon)$ consisting of a set of vertices υ and edges ε is represented by $\upsilon = \{1,\ 2,\ \ldots,\ n\}$, $\varepsilon \subseteq \{(i,j) : i,j \in \upsilon, j \neq i\}$. Each agent i is represented by a vertex, and each edge represents a communication link between a pair of agents. The neighborhood set of agent i is

$$N_i^\alpha = \{j \in \upsilon_\alpha : \|q_j - q_i\| < r, j \neq i\} \tag{21}$$

where $\|\cdot\|$ is the Euclidean norm in $\mathbb{R}^m$, and the positive constant r is the range of interaction between agents i and j. To describe the geometric model of the flock, i.e., the α–lattice, the following set of algebraic conditions should be solved Olfati-Saber (2006)

$$\|q_j - q_i\|_\sigma = d_\alpha \quad \forall j \in N_i^\alpha \tag{22}$$

where $d_\alpha = \|d\|_\sigma$, the positive constant d is the distance between neighbors i and j, and $\|d\|_\sigma$ is the σ-norm expressed by $\|z\|_\sigma = \frac{1}{\epsilon}[\sqrt{1+\epsilon\|z\|^2} - 1]$, with $\epsilon > 0$, and differentiable everywhere. From the above constraints, a smooth collective potential function can be obtained as

$$V(q) = \frac{1}{2}\sum_i \sum_{j\neq i} \psi_\alpha(\|q_j - q_i\|_\sigma) \tag{23}$$

where $\psi_\alpha(z)$ is a smooth pairwise potential function defined as $\psi_\alpha(z) = \int_{d_\alpha}^{z} \phi_\alpha(s)ds$, with $\phi_\alpha(z) = \rho_h(z/r_\alpha)\phi(z - d_\alpha)$, $\phi(z) = \frac{1}{2}[(a+b)\sigma_1(z+c) + (a-b)]$, and $\sigma_1(z) = \dfrac{z}{\sqrt{1+z^2}}$. Also, $\phi(z)$ is a sigmoidal function with $0 < a \leq b$, $c = |a-b|/\sqrt{4ab}$, to guarantee that $\phi(0) = 0$. The term $\rho_h(z)$ is a scalar bump function that smoothly varies between $[0,1]$. A possible choice for defining $\rho_h(z)$, with $h \in (0,1)$, is as follows Olfati-Saber (2006):

$$\begin{cases} 1, & z \in [0,h) \\ \dfrac{1}{2}\left[1 + \cos\left(\pi\dfrac{z-h}{1-h}\right)\right], & z \in [h,1] \\ 0, & \text{otherwise} \end{cases} \tag{24}$$

The flocking control algorithm $u_i = u_i^\alpha + u_i^\beta + u_i^\gamma$ introduced in Olfati-Saber (2006) allows avoiding obstacles, while making all agents to form an α–lattice configuration. The algorithm has three parts: u_i^α is the interaction component between two α–agents, u_i^β is the interaction component between the α–agent and an obstacle (the β–agent), and u_i^γ is a goal component consisting of a distributed navigational feedback term. In particular

$$\begin{aligned} u_i^\alpha = & c_1^\alpha \sum_{j\in N_i^\alpha} \phi_\alpha(\|q_j - q_i\|_\sigma)\mathbf{n}_{i,j} + \\ & c_2^\alpha \sum_{j\in N_i^\alpha} a_{ij}(q)(p_j - p_i) \end{aligned} \tag{25}$$

$$\begin{aligned} u_i^\beta = & c_1^\beta \sum_k \in N_i^\beta \phi_\beta(\|\hat{q}_{i,k} - q_i\|_\sigma)\hat{\mathbf{n}}_{i,k} + \\ & c_2^\beta \sum_{k\in N_i^\beta} b_{i,k}(q)(\hat{p}_{i,k} - p_i) \end{aligned} \tag{26}$$

$$\begin{aligned} u_i^\gamma = & - c_1^\gamma(q_i - q_r) - c_2^\gamma(p_i - p_r) \\ & - c_1^{\mathrm{sc}}\left(\frac{\sum_{i=1}^n q_i}{n} - q_r\right) - c_2^{\mathrm{sc}}\left(\frac{\sum_{i=1}^n p_i}{n} - p_r\right) \end{aligned} \tag{27}$$

where c_1^α, c_1^β, c_1^γ, c_1^{sc}, c_2^α, c_2^β, c_2^γ and c_2^{sc} are positive constants. The pair $(q_r,\ p_r)$ is the coordinates of a virtual leader of the MAS flock, i.e., the γ–agent which can be represented as $\{\dot{q}_r = p_r,\ \dot{p}_r = f_r(q_r, p_r)\}$. The terms $\sum_{i=1}^n q_i/n$ and $\sum_{i=1}^n p_i/n$ define the coordinates of the Center of Mass (CoM) of the MAS. The terms $\mathbf{n}_{i,j}$ and $\hat{\mathbf{n}}_{i,k}$ are vectors defined similar as in Olfati-Saber (2006) and La and Sheng (2009). The stability of the MAS flocking comes from Theorem 1 in La and Sheng (2009).

The weights of the attractive force between the MAS CoM and the reference, c_1^{sc} and c_2^{sc}, are freely set so that the CoM can converge to the reference as soon as possible. In La and Sheng (2009) the authors show that the choice of c_1^{sc}, c_2^{sc} does not affect the consensus stability or the obstacle avoidance. This is different from the choice of c_1^γ, c_2^γ which are selected less than that of c_1^β, c_2^β respectively, while c_1^β and c_2^β should be less than c_1^α and c_2^α, respectively.

Finally, $b_{i,k}(q)$ and $a_{ij}(q)$ are the elements of the heterogeneous adjacency matrix $B(q)$ and spatial adjacency matrix $A(q)$, respectively, which are described as $b_{i,k}(q) = \rho_h(\|\hat{q}_{i,k} - q_i\|_\sigma/d_\beta)$ and $a_ij(q) = \rho_h(\|q_j - q_i\|_\sigma)/r_\alpha \in [0,1]$, $i \neq j$. In these equations, $r_\alpha = \|r\|_\sigma$, $a_{ii}(q) = 0\ \forall i$ and q, $d_\beta = \|d'\|_\sigma$, and $r_\beta = \|r'\|_\sigma$. The positive constant d' is the distance between an α–agent and obstacles. The term $\phi_\beta(z)$ is a repulsive action function which is defined as $\phi_\beta(z) = \rho_h(z/d_\beta)(\sigma_1(z - d_\beta) - 1)$. Now we can define the set of β–neighbors of the i-th α–agent in a similar way to equation (21) as $N_i^\beta = \{k \in \nu_\beta : \|\hat{q}_{i,k} - q_i\| < r'\}$ where the positive constant r' is the range of interaction of an α–agent with obstacles.

Improving the effect of repulsive forces in MAS consensus and obstacle avoidance

The force emerging from the stabilization of the CoM of the MAS reduces the distance between each agent in the MAS, and also between agents and obstacles. To overcome this problem, we propose a new control action that increases the repulsion forces in case that these distances are less than the desired ones. The idea is to include compensation terms $u_{i,\mathrm{rej}}^\alpha$ and $u_{i,\mathrm{rej}}^\beta$ to u_i^α and u_i^β as follows

$$\text{if } \|q_j - q_i\| < d, \quad u_{i,new}^\alpha = u_i^\alpha + u_{i,\mathrm{rej}}^\alpha \tag{28}$$

$$\text{if } \|\hat{q}_{i,k} - q_i\| < d, \quad u_{i,new}^\beta = u_i^\beta + u_{i,\mathrm{rej}}^\beta \tag{29}$$

where $u_{i,\mathrm{rej}}^\alpha$ and $u_{i,\mathrm{rej}}^\beta$ are generate exactly as u_i^α and u_i^β, but with parameters $(c_{1,\mathrm{rej}}^\alpha, c_{2,\mathrm{rej}}^\alpha)$ and $(c_{1,\mathrm{rej}}^\beta, c_{2,\mathrm{rej}}^\beta)$, respectively. The terms $u_{i,\mathrm{rej}}^\alpha$ and $u_{i,\mathrm{rej}}^\beta$ can be seen as perturbations that disappear when the distance requirement is fulfilled, in such a way the stability is still guaranteed using Theorem 1 from La and Sheng (2009). In next section, we show by means of numerical simulations, the consequences in the MAS consensus when there is no repulsion enhanced.

In the next section we present numerical simulations showing the performance of the distributed controller.

4. SIMULATIONS

The performance of the proposed controller is demonstrated with the implementation of the numerical example

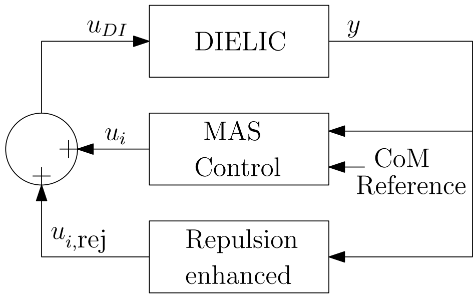

Fig. 2. Interconnection of the DIELIC with the MAS controller, together with the repulsion enhancement terms.

proposed in Baghbani et al. (2018), which consists on the stabilization and consensus of inverted pendulums. Each agent under consideration has the following dynamics

$$y = [x,\ \dot{x}]^T,\ \ddot{x} = \frac{g\sin(x) - a_p m_p l \dot{x}^2 \sin(2x)/2}{4l/3 - a_p m_p l \cos(x)^2} + \frac{a_p \cos(x)}{4l/3 - a_p m_p l \cos(x)^2} u + d \quad (30)$$

with $g = 9.81$, $m_p = 1$, $n = 10$, $l = 3$, $a_p = 1/(mp + M)$, $d(0 \leq t < 40) = 0$, $d(40 \geq t) = 2$, $\underline{x}(0) = [0.2, 0.2]^T$, and a sampling time of $T_s = 0.001$.

The ELIC tuning parameters are $r = 0.2$, $\rho = 0.075$, $K = 1$, $Q = 10$, and $Q_I = 1000$, and the reference is $x_d = \frac{\pi}{30}\sin(t)$. The weight parameters are initialized as $V_f(0) = V_g(0) = 0$, $W_f(0)$ and $W_g(0)$ take random values between -0.1 and 0.1, and $\xi(0) = 0$.

The MAS controller is tuned with the following parameters: $h = 0.2$, $c_1^\alpha = 1500$, $c_2^\alpha = 2\sqrt{c_1^\alpha}$, $c_1^\beta = 300$, $c_2^\beta = 2\sqrt{c_1^\beta}$, $c_1^\gamma = 200$, $c_2^\gamma = 2\sqrt{c_1^\gamma}$, $c_1^{sc} = 700$, $c_2^{sc} = 2\sqrt{c_1^{sc}}$, $c_{1,\text{rej}}^\alpha = 70c_1^\alpha$, $c_{2,\text{rej}}^\alpha = 70c_2^\alpha$, $c_{1,\text{rej}}^\beta = 35c_1^\beta$, $c_{2,\text{rej}}^\beta = 35c_2^\beta$.

The group of agents are tasked to follow a CoM reference in consensus mode. The numerical results in Fig. 3 show the evolution of the angular position of the 10 agents. Notice that the separation distance is successfully accomplished, despite the fact that the agents are subject to disturbances, as explained next.

The tracking of the CoM in consensus mode is shown in Fig. 4. At time $t = 23$s, an obstacle appears at position $x = 0.8$rad. Notice that, as soon as the obstacle appears, the distance between agents is successfully maintained at the desired value. The CoM state is simultaneously modified, allowing the agents to maintain the desired inter-agent separation.

As an additional test, a perturbation appears at time $t = 40$s, which simulates an uniform force in the positive x axis, and affects all the agents simultaneously. Notice from Fig. 3 that each agent rejects the perturbation and the MAS can effectively follow the CoM. The agent velocities are shown in Fig. 5. The small variations in the velocity after $t = 23$s are due to the fact that the agents perform small corrections in order to ensure the separation force (repulsion) required to fulfill the minimum distance requirements, while overcoming the effect of disturbances, and tracking the CoM.

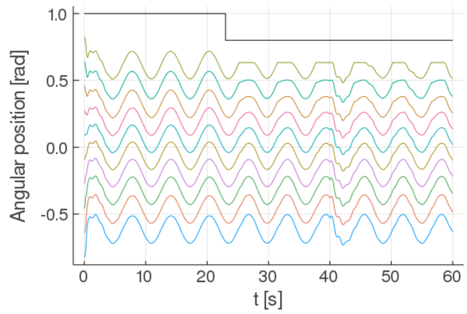

Fig. 3. Positions of a 10-agent MAS (1D agents) following a sinusoidal reference, and maintaining a security distance from a wall-type obstacle (black line).

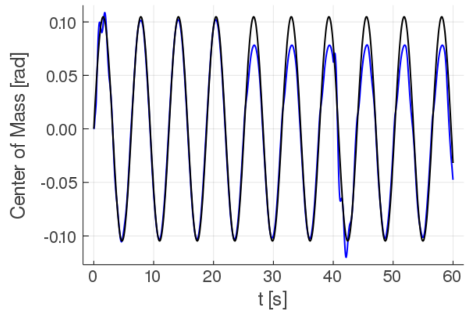

Fig. 4. Time evolution of the CoM of the MAS formation (blue) w.r.t. the desired reference (black).

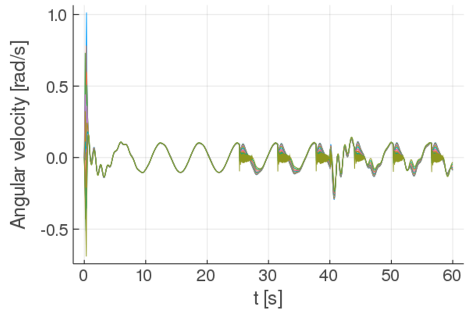

Fig. 5. Angular velocity all the agents of the MAS.

A study on how the CoM tracking force can generate a negative effect on the inter-agent repulsion force

An additional numerical simulation was conducted, but now without implementing the strategy for improvement of the repulsion force introduced in Section 3. The objective is to show that the CoM tracking force can have a negative effect on the MAS inter–agent distances when using a conventional consensus protocol.

On one hand, Fig. 6 shows the CoM tracking is successfully achieved even in the presence of the external (wall-type) perturbation. However, from Fig. 7 it can be seen that the inter-agent distance is not properly maintained (compare with the result in Fig.3). Finally, Fig. 8 shows the agents velocities. Notice each agent's velocity is stable while rejecting the perturbation. The main difference between the velocities shown in Fig. 8 and the ones shown in Fig. 5 is that in Fig. 8 the obstacle is located far from the agents. Therefore, there is no need for small correction signals to avoid collisions between the obstacle and agents.

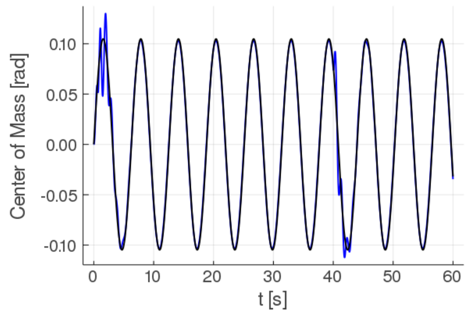

Fig. 6. CoM of the MAS without the tracking improvement from Section 3

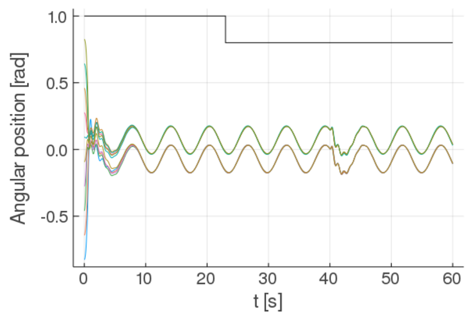

Fig. 7. Position of all the agents without the CoM tracking improvement from Section 3

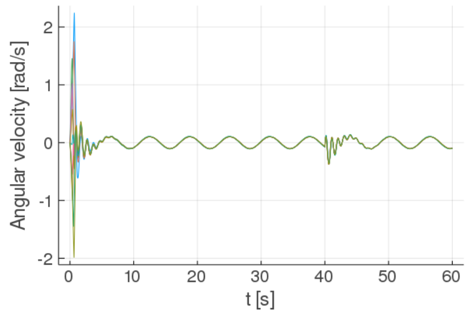

Fig. 8. Velocity of all the agents without the CoM tracking improvement from Section 3

5. CONCLUSIONS

This research introduced DIELIC: a novel performance–guaranteed consensus controller inspired by the mammalian limbic system for nonlinear MAS. The proposed framework combines a novel robust stable controller with the consensus protocol described in the seminal work in Olfati-Saber (2006).

The advantage of using the proposed DIELIC strategy to imitate a double integrator after closing the loop, relies on the fact that this formulation facilitates the implementation of MAS consensus controllers where the structure for double integrator agents is already solved. By relying on an ELIC strategy, the individual agents and also the MAS are provided with robustness to external disturbances. A novel control action was also introduced, which increases the inter–agent repulsion forces in case that these distances are less than the desired ones. The Lyapunov stability proof from Rubio Scola et al. (2020) demonstrates the stability. Numerical results consisting on the consensus control of a group of inverted pendulums under disturbances show the effectiveness and performance of the proposed approach.

Future work will be devoted to the discretization of the proposed method for real time implementation purposes, both in 2-dimensional and 3-dimensional agents.

REFERENCES

Baghbani, F., Akbarzadeh-T, M.R., and Sistani, M.B.N. (2018). Stable robust adaptive radial basis emotional neurocontrol for a class of uncertain nonlinear systems. *Neurocomputing*, 309, 11–26.

Chen, G. and Zhao, Y. (2018). Distributed adaptive output-feedback tracking control of non-affine multi-agent systems with prescribed performance. *Journal of the Franklin Institute*, 355(13), 6087–6110.

Jafari, M., Fehr, R., Carrillo, L.R.G., Quesada, E.S.E., and Xu, H. (2017a). Implementation of brain emotional learning-based intelligent controller for flocking of multi-agent systems. *IFAC-PapersOnLine*, 50(1), 6934–6939.

Jafari, M., Xu, H., and Carrillo, L.R.G. (2017b). Brain emotional learning-based intelligent controller for flocking of multi-agent systems. In *2017 (ACC)*. IEEE.

Jafari, M., Xu, H., and Carrillo, L.R.G. (2018). A neurobiologically-inspired intelligent trajectory tracking control for unmanned aircraft systems with uncertain system dynamics and disturbance. *Transactions of the Institute of Measurement and Control*, 41(2), 417–432.

La, H.M. and Sheng, W. (2009). Flocking control of a mobile sensor network to track and observe a moving target. In *2009 IEEE ICRA*, 3129–3134.

Long, X., Zhou, K., and Hou, J. (2018). Finite-time consensus for second-order multi-agent systems with disturbances by integral sliding mode algorithm based on relative information. In *2018 37th CCC*, 7112–7117. IEEE.

Lucas, C., Shahmirzadi, D., and Sheikholeslami, N. (2004). Introducing belbic: Brain emotional learning based intelligent controller. *Intelligent Automation & Soft Computing*, 10(1), 11–21.

Moren, J. (2002). *Emotion and learning: A computational model of the amygdala.* Ph.D. thesis, Lund University Cognitive Studies.

Olfati-Saber, R. (2006). Flocking for multi-agent dynamic systems: Algorithms and theory. *IEEE TAC*, 51(3), 401–420.

Pilloni, A., Pisano, A., Franceschelli, M., and Usai, E. (2013). Finite-time consensus for a network of perturbed double integrators by second-order sliding mode technique. In *52nd IEEE CDC*.

Ren, W. and Beard, R.W. (2008). Consensus algorithms for double-integrator dynamics. *Distributed Consensus in Multi-vehicle Cooperative Control: Theory and Applications*, 77–104.

Rubio Scola, I., Garcia Carrillo, L.R., and Hespanha, J. (2020). Stable robust controller inspired by the mammalian limbic system for a class of nonlinear systems. In *ACC 2020*. IEEE. Accepted.

Xu, D., Wang, X., Hong, Y., and Jiang, Z.P. (2016). Global robust distributed output consensus of multi-agent nonlinear systems: An internal model approach. *Systems & Control Letters*, 87, 64–69.